# RIS phase optimization for Near-Field 5G Positioning: ML-enhanced CRLB Minimization

#### Carla Macías\*

Department of Signal Theory and Communications
Universitat Politècnica de Catalunya
Barcelona, Spain
Email: carla.macias@upc.edu

# Montse Nájar

Department of Signal Theory and Communications Universitat Politècnica de Catalunya Barcelona, Spain Email: montse.najar@upc.edu

Abstract—This article addresses near-field localization using Reconfigurable Intelligent Surfaces (RIS) in 5G systems, where Line-of-Sight (LOS) between the base station and the user is obstructed. We propose a RIS phase optimization method based on the minimization of the Cramér-Rao Lower Bound (CRLB). This minimization itself is computationally costly, for which a data-driven method is employed with remarkable computational savings and positioning performance. The main contributions of this work are: (1) the application of machine learning (ML) to enhance CRLB minimization for RIS phase optimization; (2) an overview on RIS phases preprocessing methods to enhance deep neural networks training for the task; and (3) an end-to-end simulation of the positioning task with the presented method, showing a computational improvement without compromising positioning accuracy.

#### I. Introduction

One of the key requirements for the interaction between the digital and physical world is high-definition situational awareness, which refers to the ability of a device to determine its own location in a given environment. Indoor localization and tracking technologies are therefore crucial to achieve such a requirement [1].

The use of 5G signals yields to accuracy levels on the order of 1 meter, through the use of wide bandwidths and high carrier frequencies. Moving beyond 5G, the trend is to operate at much higher frequencies, benefiting from large available bandwidths and, therefore, achieving an even higher localization accuracy. Nonetheless, transmissions at these elevated carrier frequencies may encounter obstacles as objects obstruct the Line-of-Sight (LoS) path between transmitters and receivers [2]. The blockage of the LoS and the issues associated with Received Signal Strength (RSS) localization methods [3], [4] constitute two key challenges for the localization accuracy improvement.

With these challenges in mind, the use of Reconfigurable Intelligent Surfaces (RIS) can effectively assist the base station

\*Indicates shared first authorship.

Arnau Saumell\* *Universitat Politècnica de Catalunya*Barcelona, Spain

Email: arnau.saumell@gmail.com

#### Pau Closas

Department of Electrical and Computer Engineering
Northeastern University
Boston, Massachusetts
Email: closas@ece.neu.edu

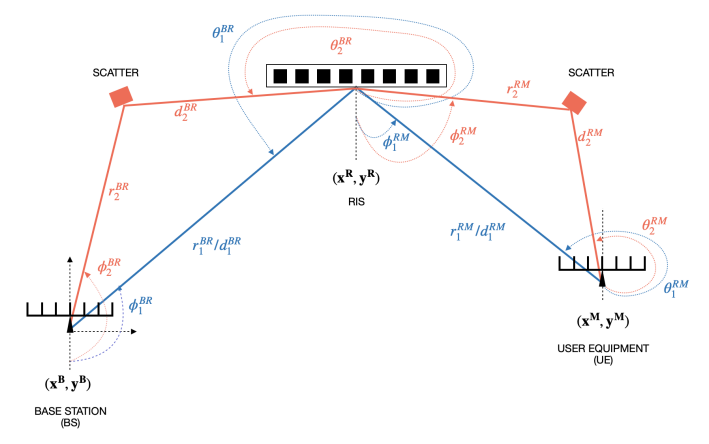


Fig. 1: Proposed architecture with the aid of a RIS in a 2D scenario where the LoS between the BS and UE is blocked.

(BS) to accomplish the user equipment's (UE) localization task, overcoming the first of the aforementioned issues [5], [6].

By introducing a RIS in our transmission framework, as shown in Fig.1, the path loss between the UE and the BS can be remarkably reduced. In addition, the RIS can modify the impinging electromagnetic waves induced by the environment, avoiding them to interfere with the transmitted signal [7]. Altogether, leads to a notable enhancement of the positioning accuracy [8].

This article delves into near-field localization using a RIS within 5G systems, focusing on scenarios where LoS communication between the BS and the UE is obstructed. [9] proposes a framework for UE localization at the BS in near-field scenario, obtaining RIS optimized phases by the derivation of the CRLB. The main goal of this article is to replicate this optimization using ML-based methods, in order to reduce its

high computational cost.

The main contributions of this article are: (1) the application of machine learning to enhance CRLB minimization for RIS phase optimization; (2) an overview on RIS phases preprocessing methods to enhance deep neural networks training for the task; and (3) an end-to-end simulation of the positioning task with the presented method.

The remainder of the paper is organized as follows. Section II introduces the problem formulation and notation. Section III presents the technical contribution of the article, the ML-based RIS phase optimization. Section IV discusses the experiments that validate the proposed methodology and Section V concludes the paper with final remarks.

#### II. BACKGROUND

## A. System Model

The architecture schema is presented in Fig.1. All components are equipped with multiple-input multiple-output (MIMO) uniform linear arrays (ULAs) with a number of elements  $N^B$ ,  $N^R$ ,  $N^M$ , for the BS, RIS and UE respectively [10].

The system model can be expressed as,

$$Y = HX + Z \tag{1}$$

where  $\mathbf{Y} \in \mathbb{C}^{N^B \times M^0}$  is the received signal,  $\mathbf{X} \in \mathbb{C}^{N^M \times M^0}$  is the Positioning Reference Signal (PRS) composed by orthogonal column pilots having  $M^0$  sequences with power P, and  $\mathbf{Z} \in \mathbb{C}^{N^B \times M^0}$  is an Additive White Gaussian Noise (AWGN) of zero mean and variance  $\sigma^2$ . The matrix  $\mathbf{H} \in \mathbb{C}^{N^B \times N^M}$  is the channel matrix, which can be expressed as

$$\mathbf{H} = \mathbf{H}^{BR} \mathbf{\Omega} \mathbf{H}^{RM} \tag{2}$$

where  $\Omega \in \mathbb{C}^{N^R \times N^R}$  is a diagonal matrix with elements  $\Theta = [\xi_1 e^{j\theta_1}, ..., \xi_{N_R} e^{j\theta_{N_R}}]$  with  $\xi_j$  and  $\theta_j$  being the magnitudes and the RIS phases, respectively (we will assume the ideal case magnitudes  $\xi_j = 1$ );  $\mathbf{H}^{BR} \in \mathbb{C}^{N^B \times N^R}$  is the channel between the BS and RIS; and  $\mathbf{H}^{RM} \in \mathbb{C}^{N^R \times N^M}$  is the channel between the RIS and UE. These channels are defined as follows:

$$\mathbf{H}^{BR} = \mathbf{A}(\phi^{BR}, r^{BR}) \operatorname{diag}(\rho^{BR}) \mathbf{A}^H(\theta^{BR}, d^{BR}) \qquad (3)$$

where  $\mathbf{A}(\phi^{BR}, r^{BR}) \in \mathbb{C}^{N^B \times L^{BR}}$ ,  $\operatorname{diag}(\rho^{BR}) \in \mathbb{C}^{L^{BR} \times L^{BR}}$  and  $\mathbf{A}(\theta^{BR}, d^{BR}) \in \mathbb{C}^{N^R \times L^{BR}}$  (with  $L^{BR}$  and  $L^{RM}$  being the number of paths between the BS and the RIS, and between the RIS and the UE respectively). The channel  $\mathbf{H}^{RM}$  can be obtain analogously.

Given that a near-field scenario is considered, the elements of the steering matrices **A** can be obtained using the Fresnel approximation of the spherical wavefront model [11] as follows,

$$a_{t,l}(\alpha_l^q, s_l^q) = e^{j(t\omega(\alpha_l^q) + t^2\gamma(\alpha_l^q, s_l^q))}$$
with 
$$\begin{cases} \omega(\alpha_l^q) = -\frac{2\pi\delta}{\lambda}\sin(\alpha_l^q) \\ \gamma(\alpha_l^q, s_l^q) = \frac{\pi\delta^2}{\lambda s_l^q}\cos^2(\alpha_l^q) \end{cases}$$
(4)

where  $\lambda$  is the wavelength,  $\delta$  is the distance between two adjacent elements in the ULA. Notice that Eq. 4 is a general expression that applies to each of the two channels. We expressed it in a compact form where superindex q can be either the BR or RM paths,  $\alpha \in \{\phi, \theta\}$  and  $s \in \{r, d\}$ .

More specifically, the parameters defining the BR channel are such that  $q=BR,\ t=b$  where  $b\in\widetilde{B},\ \widetilde{B}=[-B,\dots,B]$  and  $B\doteq\frac{(N^B-1)}{2}.$  And analogously for the RM channel.

The propagation gain of path 1 can be modeled as Finally,  $\rho_l^q$  is the propagation gain of path l, represented as,

$$\rho^q = \left(\frac{c}{4\pi(r^q + d^q)f_c}\right)^{\mu/2} F \tag{5}$$

where c as the speed of light,  $f_c$  is the carrier frequency and F represents the fading coefficient [12].

## B. Localization Algorithm

Given the system model defined in subsection II-A, the localization algorithm is based on an iterative alternating process between RIS phases and UE's position.

From the received signal  $\mathbf{Y}$  (dependant on the estimated RIS phases  $\Omega$ ), the steering angles ( $\phi_l^q$  and  $\theta_l^q$ ) and distances ( $r_l^q$  and  $d_l^q$ ) can be estimated through Compressed Sensing (CS) [13].

Subsequently, the optimized phases of  $\Omega$  are determined based on the chosen phase optimization method (see II-C). Afterwards, with the updated RIS matrix, all parameters are recomputed and the entire process is repeated until convergence. Further details on this process are presented in [9].

#### C. SNR and CRLB-Based RIS Phase Optimization

The main objective of RIS phase optimization is to improve the accuracy of the UE's position estimation by minimizing its average distortion with Euclidean distance measure [14]. In other words, it aims to minimize the position's mean square error (MSE):

$$MSE(\boldsymbol{\xi}, \hat{\boldsymbol{\xi}}) = \mathbb{E}\left[ (x^M - \hat{x}^M)^2 \right] + \mathbb{E}\left[ (y^M - \hat{y}^M)^2 \right]$$
 (6)

An approach to tackle this optimization is maximizing the signal-to-noise ratio (SNR) by aligning the phases at the BS, as done in [12]. As a result, a closed-form solution for the phases can be obtained as:

$$\begin{split} \theta_{r}^{*} = & \Big( (2M+1)(2B+1)L^{BR}L^{RM} \Big)^{-1} \sum_{b,m} \Big[ b\omega(\hat{\phi}^{BR}) \\ & + b^{2}\gamma(\hat{\phi}^{BR}, \hat{r}^{BR}) + r\omega(\hat{\theta}^{BR}) + r^{2}\gamma(\hat{\theta}^{BR}, \hat{d}^{BR}) \\ & + r\omega(\hat{\phi}^{RM}) + r^{2}\gamma(\hat{\phi}^{RM}, \hat{r}^{RM}) + m\omega(\hat{\theta}^{RM}) \\ & + m^{2}\gamma(\hat{\theta}^{RM}, \hat{d}^{RM}) \Big], \quad \forall r \in (1, \dots, N^{R}) \end{split}$$
 (7)

An alternative method is to minimize the positioning CRLB, assuming near-field scenario conditions. In comparison to the aforementioned method, this approach offers a tighter connection to the problem of minimizing the MSE [14].

Hence, the objective is to find the RIS phases that provide the minimum theoretically attainable value for the standard deviation of the positioning estimation (for unbiased estimators), i.e.

$$MSE(\boldsymbol{\xi}, \hat{\boldsymbol{\xi}}) \ge tr(\mathbf{J}_{\boldsymbol{\xi}}^{-1})$$
 (8)

where  $\boldsymbol{\xi} = \begin{bmatrix} x^M, y^M \end{bmatrix}^\top$  is the vector of unknown parameters and  $\mathbf{J}_{\boldsymbol{\xi}}$  denotes its associated Fisher Information Matrix (FIM). Such a matrix can be computed from the FIM of the parameters  $\boldsymbol{\eta} = [d^{RM}, r^{RM}, \phi^{RM}, \theta^{RM}]^\top$ , denoted as  $\mathbf{J}_n$ .

$$[\mathbf{J}_{\eta}]_{i,j} = \Psi(\eta_i, \eta_j) = \frac{P}{\sigma^2} \mathcal{R} \left\{ \operatorname{tr} \left( \frac{\partial \mathbf{\Pi}^H}{\partial \eta_i} \frac{\partial \mathbf{\Pi}}{\partial \eta_j} \right) \right\}$$
(9)

where SNR =  $\frac{P}{\sigma^2}$  and  $\Pi = \mathbf{H}^{BR} \mathbf{\Omega} \mathbf{H}^{RM} \mathbf{X}$ .

Using the transformation provided by this Jacobian matrix, we can finally obtain  $\mathbf{J}_{\xi}$  as

$$\mathbf{J}_{\xi} = \mathbf{T} \mathbf{J}_{\eta} \mathbf{T}^{\top} \tag{10}$$

where  $[\mathbf{T}]_{i,j} = \frac{\partial \eta_i}{\partial \boldsymbol{\xi}_j}$ . Hence, the final optimization problem is defined as,

$$\hat{\mathbf{\Omega}} = \underset{\mathbf{\Omega}}{\operatorname{arg\,min}} \operatorname{tr}(\mathbf{J}_{\xi}^{-1}) \ . \tag{11}$$

See [9] for further details on the derivation of this expression.

#### III. ML-BASED RIS PHASE OPTIMIZATION

Computing the CRLB minimization is computationally expensive. Hence, in order to replicate this optimization process relieving the computational burden, these optimal phases are computed through a neural network. The model used is a Multi-Layer Perceptron which is fed with the standardized positions, and it outputs the corresponding  $N^R$  phases in the  $[0,2\pi]$  range.<sup>1</sup>

To train the model, an extensive dataset of positions and optimal phases has been computed, using the original approach of minimizing the CRLB function.

#### A. Phase Distribution Smoothing

Recall that the dataset phases have been computed through the minimization of the CRLB function. This optimization process usually leads to local optima, which creates certain noise on the phases distribution across the grid of positions. Such a phenomena is illustrated in Fig. 2 for a single phase. Hence, in order to ensure a smoother and more stable training of our model we have introduced a smoothing process over the distribution of each phase individually. In fact, this theoretical reasoning is actually supported by empirical evidence as results have proven in the next section.

Two potential smoothing processes have been studied:

• *Uniform smoothing*: application of a median filter with a squared kernel over the distribution of each individual

 $^1 \text{The}$  model is a 5-layer MLP, with ReLU intermediate layers and Dropout layers with value 0.1. The output layer of the MLP is a Sigmoid with a  $2\pi$  product factor, in order to ensure outputs in the desired range. The model was trained for 1000 epochs, and we used an Adam optimizer and the Cosine Annealing scheduler. The initial learning rate value ( $l_r=0.001$ ) and the L2 regularization factor ( $l_2=10^{-5}$ ) have been optimized using Bayesian Optimization.

- phase when taken as a grid according to their associated positions.
- Conditional smoothing: similarly to the previous process, apply a median filter over the distribution of phases. However, in this case the resulting filtered phase value will only be taken for those positions in which the resulting value differs from more than a threshold k with respect to its original value. The idea here is to correct only those values that are clear outliers, and preserve the details of the original phase distribution.

Both the kernel size (kernel\_size= 3) and the threshold value (k=1) have been chosen based on a qualitative analysis across the plots of each individual phase, seeking an optimal trade-off between outlier removal and detail preservation. Fig. 2 depicts an example of this process for a single phase.

Notice that, since we are working with modular data (angles), distances between phases are always computed as the shortest distance in both directions, i.e.,

$$\theta_1 - \theta_2 := \min(|\theta_1 - \theta_2|, 2\pi - |\theta_1 - \theta_2|). \tag{12}$$

# IV. RESULTS

#### A. Training Results

As depicted in the previous section, this work defines 3 types of phase preprocessing methods before training the MLP (no-preprocessing, uniform smoothing and conditional smoothing). The quantitative comparison of the training results for each kind of data is summarized in Table I. Notice that, no matter whether the phases have been previously preprocessed, to evaluate the prediction accuracy of each framework we will always compare the predicted phases with the original non-processed ones (given that these are theoretically the ones we aim to resemble).

Preprocessing	MAE (rad)	RMSE (rad)
No smooth.	0.643	0.978
Uniform smooth.	0.505	0.765
Conditional smooth.	0.508	0.769

TABLE I: Mean Absolute Error (MAE) and Root Mean Square Error (RMSE) between the original phases and the predicted ones by the MLP trained with each preprocessing method. Distances between phases are computed according to Eq. 12.

In terms of qualitative analysis, Fig. 3 shows how discontinuities in the original phase distribution worsen the MLP predictions (*MLP Prediction - Original Phases* plot in Fig. 3). For some close positions in the grid, we appear to have hard-to-generalize phase changes (i.e. outliers) and so the MLP proves to be unable to track these changes during training. The result is an averaged prediction as shown in Fig. 3. Such a result backs our original hypothesis motivating the use of preprocessed phases for the training.

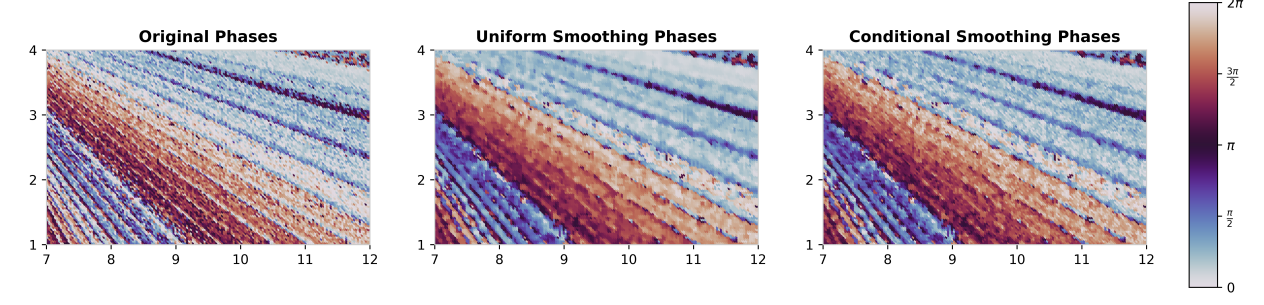


Fig. 2: Distribution of the 7<sup>th</sup> phase over the grid of positions. (1) *Original phases* are the non-processed phase values for each position according to the CRLB minimization, (2) *Uniform Smoothing Phases* are the uniformly smoothed phase values, and (3) *Conditional Smoothing Phases* are the conditionally smoothed phase values.

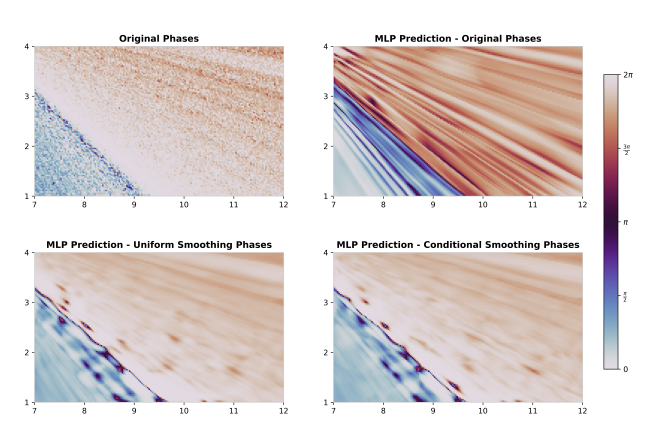


Fig. 3: Distribution of the 1<sup>st</sup> phase over the grid of positions. (1) *Original phases* are the raw phases according to the CRLB minimization, (2) *MLP Prediction - Original Phases* are the phases predicted by the model trained with the raw phases, (3) *MLP Prediction - Uniform Smoothing Phases* are the phases predicted by the model trained with the uniformly smoothed phases, and (4) *MLP Prediction - Uniform Smoothing Phases* are the phases predicted by the model trained with the conditionally smoothed phases.

## B. Positioning Error

This subsection provides a quantitative analysis on the position estimation accuracy, focusing on the comparison between methods and their respective associated computational costs. We will distinguish six different frameworks based on the RIS phases optimization method used:

- Random phases: non-optimized (random) phases.
- *Max. SNR method*: phases optimized maximizing the SNR (as proposed in [12]).
- *Min. CRLB method*: phases optimized minimizing the CRLB (as proposed in [9]).
- *MLP Original Phases*: ML-based optimization using the raw phases.
- *MLP Uniform Smoothing*: ML-based optimization using uniform smoothing on the phases.
- MLP Conditional Smoothing: ML-based optimization using conditional smoothing on the phases.

The fixed parameters throughout the whole simulation are:  $\mathbf{x}^B = [0,0], \mathbf{x}^R = [5,5], \mathbf{x}^M = [9,2.5], N^B = 51, N^M = 21, N^R = 40, f_c = 28$  GHz,  $\mu = 3$  and  $M^0 = 64$ . In addition, to obtain the transmitted SNR, thermal noise is considered  $(\sigma^2 = B_t K T_k$ , with  $B_t = 10$  MHz, K being the Boltzmann constant and  $T_k = 290$  K).

Fig. 4 depicts a comparative analysis of the six methods in terms of the evolution of the RMSE throughout the iterations of the positioning algorithm defined in II-B. As expected, *Random Phases* and *Max. SNR method* stand at a high magnitude positioning error, on the order of 5 and 2 meters respectively. In relation to the ML-based methods, these accomplish an outstanding positioning accuracy comparable to the baseline method (i.e. *Min. CRLB*). Especially, the conditional smoothing preprocessing almost reaches this baseline error. See Table II for a more detailed view onto the respective positioning errors.

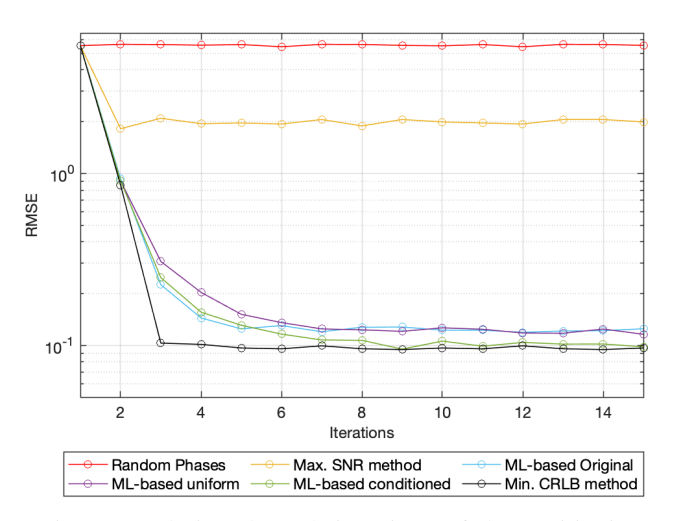


Fig. 4: Evolution through iterations of the positioning RMSE for the six optimization methods. Due to the high variability on each repetition, 1000 Monte Carlo simulations have been performed for each framework.

Optimization method	Positioning RMSE (m)
Random phases	5.551
Max. SNR method	1.992
MLP Original Phases	0.125
MLP Uniform Smoothing	0.116
MLP Conditional Smoothing	0.098
Min. CRLB method	0.096

TABLE II: Comparison of the positioning RMSE after 15 iterations for the simulations depicted in Fig. 4.

#### C. Computational Cost

Table III shows the computation time comparison between the novel methods and the *Min. CRLB method*. Notice that, since all the ML-based methods are essentially the same in terms of computational cost (they are simply differently trained MLPs), they are all grouped under *ML-based methods*. These results show how the proposed framework clearly outperforms the *Min. CRLB method* in terms of computation time. In fact, the ML-based methods take only 1.5% of the total time spent by the *Min. CRLB method*.

Notice that the cost of the dataset generation and the MLP training are neglected, since this is a one-off process. Hence, the only computation involved during the positioning algorithm is a single network forward propagation for each iteration.

Minimization method	Time (s)
Min. CRLB method	3227
ML-based methods	49

TABLE III: Comparison between *Min. CRLB method* and ML-based methods, on the time spent to compute the optimized RIS phases. Times are obtained for a 15-iteration positioning algorithm and 50 Monte Carlo simulations.

#### V. CONCLUSION

This article proposes an ML-based framework to replicate optimal RIS phase computation according to CRLB minimization, in the context of 5G positioning systems in a near-field scenario. The proposed method shows a substantial computational gain with respect to the baseline method (i.e. phase optimization through CRLB function minimization), without compromising the positioning error. In addition, two phase pre-processing methods have been introduced in order to enhance the MLP training, showing a slight improvement in both training and positioning error.

Although the gain in computational cost is notable, the presented methods still have potential for improvement in terms of achievable positioning accuracy. One of the main sources of this gap comes from the stochasticity associated to the CRLB function minimization during the computation of the dataset phases. Hence, one of the key areas for further enhancement would be the development of better pre-

processing methods, which can serve as additional refinements to the CRLB-optimized phases.

#### ACKNOWLEDGMENTS

The UPC authors are within the Signal Processing and Communications Group at UPC recognized as a consolidated research group by the Generalitat de Catalunya through 2021 SGR 01033. This publication is part of the project ROUTE56 with grant PID2019-104945GB-I00 funded by MCIN/AEI/ 10.13039/501100011033 and the project 6-SENSES with grant PID2022-138648OB-I00 funded by MCIN/AEI/ 10.13039/501100011033 and by ERDF A way of making Europe. This work has been partially supported by the National Science Foundation under Awards ECCS-1845833 and CCF-2326559.

#### REFERENCES

- [1] Davide Dardari, Pau Closas, and Petar M Djurić. Indoor tracking: Theory, methods, and technologies. *IEEE Transactions on Vehicular Technology*, 64(4):1263–1278, 2015.
- [2] Xilong Pei, Haifan Yin, Li Tan, Lin Cao, Zhanpeng Li, Kai Wang, Kun Zhang, and Emil Björnson. RIS-Aided Wireless Communications: Prototyping, Adaptive Beamforming, and Indoor/Outdoor Field Trials. IEEE Transactions on Communications, 69(12):8627–8640, 2021.
- [3] Ali Yassin, Youssef Nasser, Mariette Awad, Ahmed Al-Dubai, Ran Liu, Chau Yuen, Ronald Raulefs, and Elias Aboutanios. Recent advances in indoor localization: A survey on theoretical approaches and applications. IEEE Communications Surveys Tutorials, 19(2):1327–1346, 2017.
- [4] Haobo Zhang, Hongliang Zhang, Boya Di, Kaigui Bian, Zhu Han, and Lingyang Song. Metalocalization: Reconfigurable intelligent surface aided multi-user wireless indoor localization, 2023.
- [5] Marco Di Renzo, Alessio Zappone, Merouane Debbah, Mohamed-Slim Alouini, Chau Yuen, Julien de Rosny, and Sergei Tretyakov. Smart radio environments empowered by reconfigurable intelligent surfaces: How it works, state of research, and road ahead, 2020.
- [6] Cunhua Pan, Gui Zhou, Kangda Zhi, Sheng Hong, Tuo Wu, Yijin Pan, Hong Ren, Marco Di Renzo, A. Lee Swindlehurst, Rui Zhang, and Angela Yingjun Zhang. An Overview of Signal Processing Techniques for RIS/IRS-Aided Wireless Systems. *IEEE Journal of Selected Topics in Signal Processing*, 16(5):883–917, 2022.
- [7] Miguel Dajer, Zhengxiang Ma, Leonard Piazzi, Narayan Prasad, Xiao-Feng Qi, Baoling Sheen, Jin Yang, and Guosen Yue. Reconfigurable intelligent surface: Design the channel a new opportunity for future wireless networks, 2020.
- [8] Jiguang He, Henk Wymeersch, Long Kong, Olli Silvén, and Markku Juntti. Large intelligent surface for positioning in millimeter wave mimo systems, 2019.
- [9] Carla Macias, Montse Nájar, and Pau Closas. RIS phase optimization for Near-Field 5G Positioning: CRLB Minimization. Valencia, Spain, Sep. 2024. IEEE.
- [10] Jiguang He, Henk Wymeersch, and Markku Juntti. Channel Estimation for RIS-Aided mmWave MIMO Systems via Atomic Norm Minimization. *IEEE Transactions on Wireless Communications*, 20(9):5786–5797, 2021.
- [11] Sen Li, Bing Li, Bin Lin, Xiaofang Tang, and Rongxi He. Sparse reconstruction based robust near-field source localization algorithm. Sensors, 18(4), 2018.
- [12] Omar Rinchi, Ahmed Elzanaty, and Mohamed-Slim Alouini. Compressive Near-Field Localization for Multipath RIS-Aided Environments. IEEE Communications Letters, 26(6):1268–1272, 2022.
- [13] Dror Baron, Michael B. Wakin, Marco F. Duarte, Shriram Sarvotham, and Richard Baraniuk. Distributed compressive sensing. ArXiv, abs/0901.3403, 2009.
- [14] Ahmed Elzanaty, Anna Guerra, Francesco Guidi, and Mohamed-Slim Alouini. Reconfigurable intelligent surfaces for localization: Position and orientation error bounds. *IEEE Transactions on Signal Processing*, 69:5386–5402, 2021.